REVIEW ON REMOTE SENSING OF THE SNOW COVER AND ON METHODS OF MAPPING SNOW

1. INTRODUCTION

Snow is a form of precipitation, but, in hydrology it is treated somewhat differently because of the lag between when it falls and when it produces runoff, groundwater recharge, and is involved in other hydrologic processes. The hydrologic interest in snow is mostly in mid- to higher latitudes and in mountainous areas where a seasonal accumulation of a snowpack is followed by an often lengthy melt period that sometimes lasts months. During the accumulation period there is usually little or no snowmelt. Precipitation falling as snow (and sometimes rain) is temporarily stored in the snowpack until the melt season begins. The hydrologist generally wants to know how much water is stored in a basin in the form of snow. The hydrologist will also be concerned with the areal distribution of the snow, its condition and the presence of liquid water in it. In general, all these indicators of snow are difficult to measure and are likely to vary considerably from point to point, especially in mountainous terrain.

Remote sensing offers a new and valuable tool for obtaining snow data for predicting snowmelt runoff. Historically, snow data have been obtained manually by means of snow courses, which are extremely labour intensive, expensive and potentially dangerous. Even when available, snow course data represent only a point and, at best, can only be used as an index of available snow water content. Recent use of telemetering of snow pillow and storage gauge measurements of precipitation have reduced the need for some fieldwork but have not overcome the problem of the point measurements of snow. That is, although measurements are automated, there is still the problem that a single point measurement may or may not be representative of a large area or basin. From a remote sensing perspective, snow cover is one of the most readily identifiable measures of water resources from aerial photography or satellite imagery. Present operational satellite systems are limited to determining only the area of snow cover, snow depth and snow water equivalent; snow physical parameters cannot be measured directly by these systems. However, it will be shown in the following sections that there is a capability for estimating these now from research instruments, and it appears that future operational systems will also provide very important snow hydrology data. A more complete description of remote sensing of snow can be found in Hall and Martinec (1985) and in Engman and Gurney (1991).

Table 1 Sensor band responses relative to various snowpack properties (Rango, 1993)

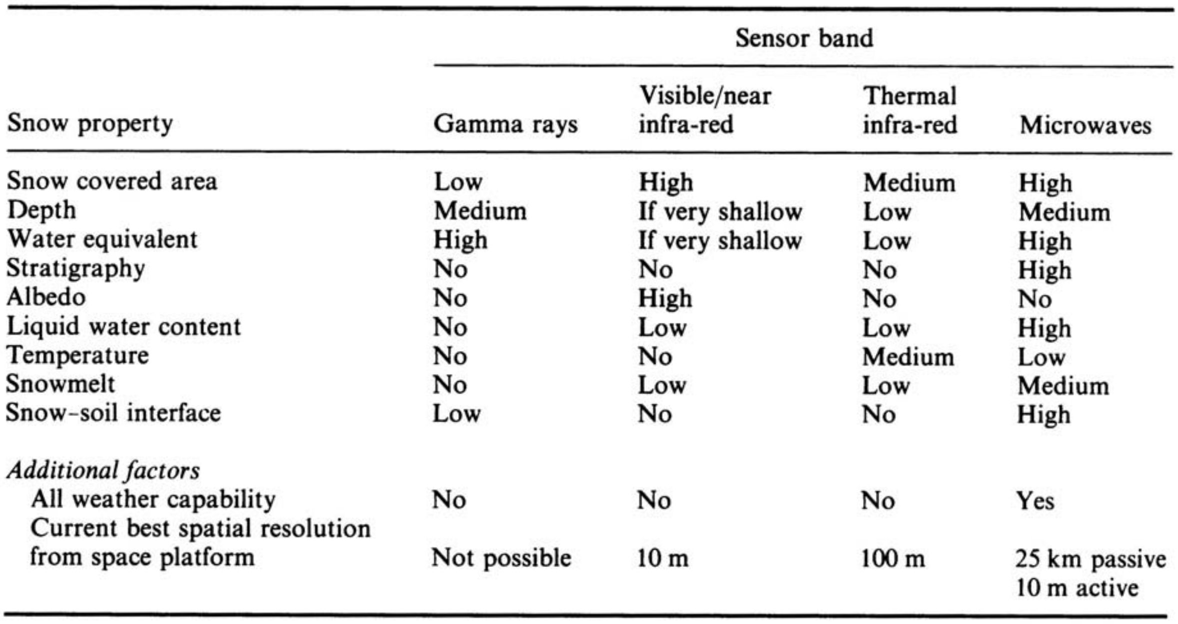

Snow property	Sensor band Gamma rays	 Visible/near infra-red	 Thermal infra-red	 Microwaves
Snow covered area	Low	High	Medium	High
Depth	Medium	If very shallow	Low	Medium
Water equivalent	High	If very shallow	Low	High
Stratigraphy	No	No	No	High
Albedo	No	High	No	No
Liquid water content	No	Low	Low	High
Temperature	No	No	Medium	Low
Snowmelt	No	Low	Low	Medium
Snow-soil interface	Low	No	No	High
Additional factors				
All weather capability	No	No	No	Yes
Current best spatial resolution from space platform	Not possible	10 m	100 m	25 km passive 10 m active

2 GENERAL APPROACH

Just about all regions of the electromagnetic spectrum can provide useful information about the snowpack and its condition. Ideally, we would like to know the areal extent of the snow, its water equivalent, and the "condition" or grain size, density and presence of liquid water. Although one region of the spectrum can provide all these properties, certain regions of the spectrum can be used to measure individual properties. Table 1 (Rango, 1993) summarizes some of the sensor responses to snowpack properties. Each of the remote sensing approaches will be addressed below, starting with the technique at the shortest wavelength.

2.1 GAMMA RADIATION

The water content of some snowpacks can be measured with low-flying aircraft carrying sensitive gamma radiation detectors. This method takes advantage of the natural emission of low-level gamma radiation from the soil. Naturally occurring radioisotopes of potassium, uranium and thallium can be found in a typical soil. Aircraft passes over the same flight line before and during snow cover measure the attenuation resulting from the snow layer which is empirically related to an average snow water equivalent for that site (Carroll and Vadnais, 1980). This approach is limited to low aircraft altitudes (approximately 150 m) because the atmosphere attenuates a significant portion of the radiant energy. This restriction effectively limits the use of gamma detection to relatively flat areas, and because of safety considerations it cannot be used in mountainous areas. Also, this approach has been limited for the most part to non-forested areas because the effect of forest biomass is to attenuate the radiation signal (Glynn *et al.*, 1988). However, past work by Carroll and Carroll (1989) suggests a means of correcting for the downward bias in measured snow water equivalent by making a correction that is based on the amount of biomass and the type of radiation. In addition, because the gamma energy is relatively low, the maximum depth of snow water equivalent is limited to about 30-40 mm and interpretation of the data can be difficult if the background soil moisture changes during the season (Vershinina, 1985). However, Carroll and Vose (1984) have reported measurements in a forest environment with a snow water equivalent of 480 mm. In the NOAA operational airborne gamma radiation snow water-mapping programme, procedures for correcting for the soil moisture were included in the system (Carroll and Carroll, 1989). This operational programme flew over 1400 flight lines in the United States and Canada (Carroll and Carroll, 1989).

2.2 VISIBLE/NEAR INFRARED

The albedo of the snow surface is the property most easily measured by remote sensing. Albedo, A, is defined as

$$A = \text{Reflected solar radiation/Incoming solar radiation} \tag{1}$$

Typically, new snow will have an albedo of 90% or more whereas older snow that has been weathered and has accumulated dust and litter can have an albedo as low as 40% (Foster *et al.,* 1987). The reflectivity depends upon snow properties such as the grain size and shape, water content, surface roughness, depth and presence of impurities. The reflectivity of new snow decreases as it ages in both the visible and infrared regions of the spectrum; however, the decrease is more pronounced in the infrared region. This increased sensitivity in the infrared region is caused by the increasing grain size of the snow which results from melting and refreezing. For the most part, decreased reflectivity in the visible region can be attributed to contaminants such as dust, pollen and aerosols.

Most current snowmelt models use either point snow course estimates of the snowpack or the total area of the snowpack. In the latter case there is usually an implicit assumption that the snow cover area and its changes are somehow consistently related to the snow water equivalent in the basin. Through careful analysis of satellite images or aerial photography, snow can be identified and the boundaries of the snow/no-snow areas accurately located. However, a certain amount of subjective interpretation may be necessary to identify and separate the effects of shadows and forests.

In non-forested terrain, all areas with continuous brightness distinctly greater than the normal dark background, and that have been assured to be cloud free, should be mapped as snow areas. The snow line that encloses these areas can be assumed to represent accumulated snow depths of 2.5 cm (Bowley *et al.,* 1981) or more. Areas on imagery that appear mottled (alternating dark and light reflectance) can be mapped as areas of between zero and 2.5 cm of snow depth. In mountainous terrain, the snow line is mapped at the edge of the brighter tone without regard to brightness variations resulting from forest effects or mountain shadow.

Snow can readily be identified and mapped with the visible bands of satellite imagery because of its high reflectance in comparison with no-snow areas. Generally, this means selecting the NOAA

VHRR visible channel, Landsat MSS channels 4 or 5, SPOT, or Landsat TM channels 2 and 4. If there is a choice of bands, it is better to choose a spectral band closer to the infrared region because at higher sun angles the Landsat MSS band 4 and TM band 1 and other bands near the blue region may be near saturation, causing a loss of detail in identifying snow and no-snow areas. Although snow can be detected at longer wavelengths, that is in the near infrared, the contrast between a snow and a no-snow area is considerably lower than with the visible region of the spectrum. However, the contrast between clouds and snow is greater in Landsat TM Band 5 (1.57-1.78 μm*)* and this serves as a useful discriminator between clouds and snow (Dozier, 1984).

2.3 THERMAL INFRARED

Thermal data are perhaps the least useful of the common remote sensing products for measuring snow and its properties. In order to determine snowpack temperatures the spectral emissivity of the snow must be known. This in turn requires knowledge of liquid water content and the grain size as well as other factors. In spite of these limitations, thermal data can be useful for helping identify snow/no-snow boundaries. Thermal infrared data are also useful for discriminating between clouds and snow with AVHRR data because the 1.57-1.78 μm band is not available on this sensor.

The emissivity of snow approaches that of a black body at the 10.5—12.5 μm atmospheric window. Griggs (1968) has shown that melting snow can have an emissivity as high as 99%, whereas the emissivity for no-snow areas is typically 95% or less.

2.4 MICROWAVE

Microwave remote sensing provides several advantages not offered by other satellite sensors. This is because the microwave data can provide information on the snowpack properties of most interest to hydrologists; that is, snow cover area, snow water equivalent (or depth) and the presence of liquid water in the snowpack which signals the onset of melt (Kunzi *et al.,* 1982). Snow on the earth’s surface is, in simple terms, an accumulation of ice crystals or grains, resulting in a snowpack which over an area may cover the ground either completely or partly. The physical characteristics of the snowpack determine its microwave properties; microwave radiation emitted from the underlying ground is scattered in many different directions by the snow grains within the snow layer, resulting in a microwave emission at the top of the snow surface being less than the ground emission. Properties affecting microwave response from a snowpack include: depth and water equivalent, liquid water content, density, grain size and shape, temperature and stratification as well as snow state and land cover. The sensitivity of the microwave radiation to a snow layer on the ground makes it possible to monitor snow cover using passive microwave remote sensing techniques to derive information on snow extent, snow depth, snow water equivalent (SWE) and snow state (wet/dry). Because the number of scatterers within a snowpack is proportional to the thickness and density, SWE can be related to the brightness temperature of the observed scene (Hallikainen and Jolma, 1986); deeper snowpacks generally result in lower brightness temperatures. Active microwave observations of the snowpack are very sparse and almost non-existent, especially around 10 cm and lower wavelengths which are ideal for snow. Most data relevant to active microwave remote sensing of snow have been acquired from truck or tower systems. Preliminary results by Stiles *et al.* (1981), Matzler and Schanda (1983) and Rott (1986) indicate that the active microwave region has a potential similar to the passive microwave region. The analysis of active microwave data, however, is more complex than passive data because of the confusion caused by the effect of surface characteristics (including soils) and geometry considerations on the reflected radar wave. A considerable advantage of the active microwave approach is an improved resolution capability (of about 10 m from space) when compared with the passive.

3 SNOW MAPPING

The aerial extent of snow cover can be determined through various remote sensing techniques. Snow cover area by itself is of little value for predicting snowmelt runoff because it provides no information on the depth or water equivalent. However, useful empirical relationships can be developed for specific basins and the temporal nature of some remote sensing data allow the inference of the rate of melt. Leaf (1969) used aerial photographs to develop relationships between snow cover and accumulated runoff for Some Colorado watersheds. Sequential photographs showing snow cover depletion were used to help estimate the timing and magnitude of snowmelt peaks.

In the mid-1960s, snow was successfully mapped from space on a weekly basis following the launch of the Environmental Science Service Administration (ESSA-3) satellite which carried the Advanced Vidicon Camera System (AVCS) that operated in the spectral range of 0.5 - 0.75 µm with a spatial resolution at nadir of 3.7 km. The National Oceanographic and Atmospheric Administration (NOAA) has measured snow cover on weekly basis in the Northern Hemisphere since 1966 using a variety of sensors, including the Scanning Radiometer (SR), Very High Resolution Radiometer (VHRR) and the Advanced Very High Resolution Radiometer (AVHRR) (Matson *et al.*, 1986; Matson, 1991). The current NOAA product is a daily snow-cover product (Ramsay, 1998).

Two important databases exist for investigations of spatial and temporal variability in hemispheric and global snow cover: the weekly National Oceanic and Atmospheric Administration (NOAA) visible satellite-based snow-cover analysis from 1972 (Robinson *et al.,* 1993), and Scanning Multispectral Microwave Radiometer (SMMR) and Special Sensor Microwave/Imager (SSM/I) passive microwave brightness temperature data from 1978, which can be used to derive information on snow extent (Chang *et al.,* 1987), depth (Foster *et al.,* 1984), and snow-water equivalence (Goodison, 1989; Chang *et al.,* 1991). The spatial and temporal character of these two data sets is relatively coarse (190.5-km polar stereographic grid and 1/week for the NOAA data set, and ~25-km resolution and 1/day for the passive microwave data) but this is sufficient for monitoring key properties such as snow extent, dates of snow-cover onset and disappearance, and peak accumulation, which are known to be important indicators of change (Barry *et al.,* 1995).

The Moderate Resolution Imaging Spectroradiometer (MODIS) is a 36-channel visible to thermal-infrared sensor that was first launched as part of the Earth Observing System (EOS) Terra payload on 18 December 1999. A second MODIS was launched as part of the payload on the Aqua satellite on May 4, 2002. A variety of snow and ice products is produced from the MODIS sensors, and the products are available at a variety of spatial and temporal resolutions as shown in the table below. The MODIS snow product suite begins with a 500-m resolution, 2330-km swath snow-cover map which is then gridded to a sinusoidal grid. The standard MODIS daily global fractional snow cover (FSC) climate modeling grid (CMG) map product is generated at 0.05° resolution (about 5 km at the equator).

3.1 CONFUSION FACTORS

When mapping snow cover there are several possible features of the imagery which must be considered in order to prevent misidentification of snow or no-snow areas. With experience, techniques have been developed to overcome some of the possibilities of misinterpretation because of the following confusion factors.

1. *Clouds.* Cloud tops exhibit a very bright reflectance in the visible bands that is often indistinguishable from snow. Differentiating between clouds and snow is one of the major problems in the use of satellite data for snow mapping. An experienced user will use some or a combination of terrain features, pattern recognition, uniformity of reflectances, the presence of shadows (either from terrain features or clouds) and scene stability with time. Snow can be distinguished from clouds by using a near-infrared channel around 1.6 μm because the cloud reflection will be bright in this region but the snow will be dark (Crane and Anderson, 1984; Dozier, 1984).
2. *Forest cover.* Forested areas can consist of everything from dense conifers to less dense deciduous forests, to sparse range-type vegetation. The reflectance from these areas will be considerably darker than non-forested areas even with substantial depths of snow because the snow will tend to filter through the forest canopy. The challenge is to determine the snow-covered areas when they may not be directly detectable. This generally requires a great deal of experience and familiarity with the area and the use of all concomitant information available (i.e. land use surveys, topographic maps, non-snow imagery, etc.). Timber cuts, roads, streams, lakes and other open land can be used because they would be highly reflective under snow cover. Digital enhancement of data can also sometimes be used if the forest cover is incomplete or sparse.
3. *Shadows.* During the winter, sun angles are generally low and the resulting northern hemisphere terrain shadows on north-facing slopes may be difficult to distinguish from bare, south-facing slopes. Topographic maps and summer imagery may help in the

interpretation. In shadow areas, snow may be distinguished from rocks or soil by selecting a threshold brightness for automated discrimination (Dozier and Marks, 1987).

4. *Rocks.* During the melt period, highly reflecting bare rock may be difficult to distinguish from late season snow. As above, summer imagery and topographic maps, as well as vegetation patterns, can help in the differentiation.

4 CURRENT APPLICATIONS

Different approaches for determining snow area, water equivalent and snow properties have been developed. These have been driven for the most part by the availability of data from existing satellites or from experimental aircraft and truck programmes. This section discusses a number of examples, some of which are operational and others still considered experimental or developmental.

4.1 SNOW COVER AREA

Snow cover area is not the ideal description of a snowpack. A hydrologist would like to have water equivalent, depth and density information, as well as the snow cover area, to make accurate estimates of snowmelt runoff. Fortunately, research has demonstrated a very good relationship between runoff and snow cover area for many basins.

Snow cover can be detected and monitored with a variety of remote sensing devices. The greatest number of applications have been found in the VNIR region of the electromagnetic spectrum. Because of Landsat and SPOT frequency of observation problems, many users have turned to the NOAA polar orbiting satellite with the AVHRR, which has a resolution of about 1km in the 0.58–0.68 lm red band. The frequency of coverage is twice every 24 h (one daytime pass and one nighttime pass). The major problem with the NOAA-AVHRR data is that the resolution of 1km may be insufficient for snow mapping on small basins. Data from the MODIS instrument on NASA’s EOS satellites with 250 m resolution in two visible bands will partially alleviate this problem.

In an early application of satellite data, Rango *et al.* (1977) used simple photointerpretation techniques to map snow cover areas in the Indus and Kabul river basins in Pakistan. Their approach was to use a simple regression between the percentage of snow cover in the basins from 1 to 20 April and the April-July streamflow. The results demonstrated the usefulness of satellite-derived runoff estimates, especially for remote and data-sparse regions of the world. This work was extended (Dey *et al.,* 1983) with an additional 6 years of data. The additional data improved the regression for the Kabul River but decreased it for the Indus River. Such results point out the inherent weakness of simple regression models representing complex processes. On the other hand, in data-sparse regions there are seldom many alternative approaches.

Landsat imagery was used to determine snow cover areas for six basins in Colorado, USA, over the period of 1973 to 1978. Shafer and Leaf (1979) concluded that the satellite imagery was of sufficient quality to monitor the snow cover area accurately. They also concluded that forecast error can be reduced by the order of 10% by using snow cover data derived from the satellite.

Aircraft and Landsat snow cover data were combined to form a long-term database for predicting runoff for basins in California. Two areas were studied by comparing snow cover area's with conventional snow data and by incorporating snow cover areas into the State's forecasts (Brown *et al.,* 1979). The results indicated a potential improvement in forecast accuracy by using snow cover area, particularly in areas where precipitation and snow course data are limited. The Kings River basin is much more predictable, in the sense of having a more uniform area-elevation distribution of snow, than the Kern River basin and its standard estimated error is relatively small. On the other hand, the procedural error for the Kern River is relatively large and the addition of snow cover data reduces this error.

NASA, in cooperation with several federal and state water resource agencies in the USA, conducted an applications systems verification and transfer (ASVT) study on the effectiveness of satellite-derived snow cover data for operational forecasting (Rango, 1980). Both empirical and short-term models were tested. Three years of testing in three California basins resulted in a reduction in the forecast errors of between 10 and 15%. In modelling studies of the Boise River in Idaho, USA, the use of satellite snow cover data reduced the 5-day forecast error by 9.6%. These results were extrapolated to estimate the benefits that would be possible through increased forecast accuracies in the 11 western states in the USA. Based on a 1980 dollar and an assumed 6% improvement in forecast accuracy, the benefits would include more than $10 million dollars from improved hydropower predictions and $28 million in irrigation water forecasting. A benefit/cost ratio was calculated to be an impressive 75 : 1 (Castruccio *et al.,* 1980). However, this figure did not consider the cost of satellite development and launch, and it also did not anticipate any improvement in satellites, models or interpretation systems.

Satellite data have been used for determining snow cover area in Norway for forecasting snowmelt runoff and managing the production of hydroelectric power (Ostrem *et al.,* 1981). These researchers have developed a method for using NOAA and TIROS data for measuring the remaining snow and to predict the corresponding snowmelt runoff volume for a number of Norwegian high mountain basins. The method is limited to essentially vegetation-free areas and only after roughly 20% of the basin is snow free. Such results, although empirical, can be developed for many basins.

The question of spatial resolution of remotely sensed data necessary to achieve satisfactory results when mapping snow cover has been addressed by Rango *et al.* (1983). Their results are summarized in Table 1.2. Since their study, SPOT and MODIS data have become available, and we might expect the usefulness of these data sets to fall between the orthophoto and Landsat TM (SPOT) and between Landsat MSS and NOAA AVHRR (MODIS).

Rango *et al.* (1979) reported data that showed a fairly good inverse relationship between snow accumulation and brightness temperature from ESMR-6 for a relatively deep snow site in North Dakota, USA. However, a similar analysis for an Indiana site in which the snow cover never exceeded 12.5 cm was not nearly as strong. Thus, it appears that shallow snow cover may not be detectable with passive microwave but that there may be a threshold above which these systems can determine snow cover and possibly the actual depth. In addition, once the snow begins to melt the emissivity of melting snow and bare ground are very similar.

Table 1 Characteristics of various remote sensing data used for snow cover mapping (Rango *et al.,* 1983)

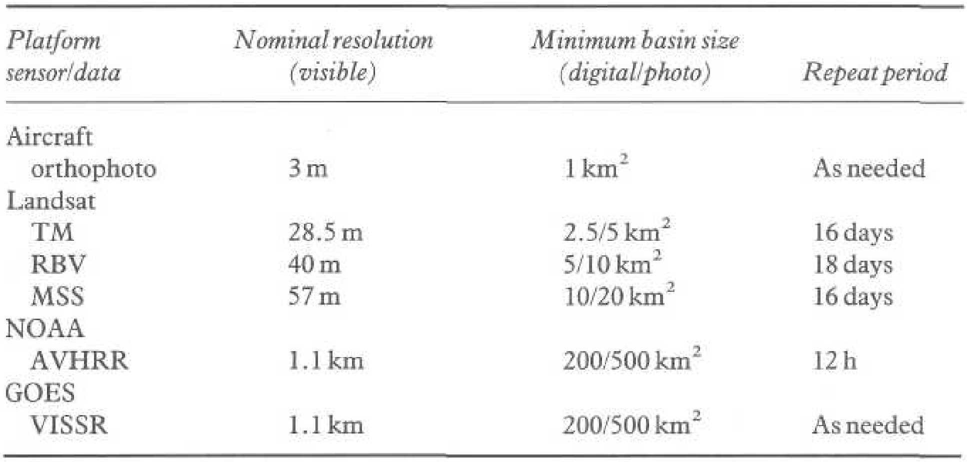

Platform sensor/data	*Nominal resolution (visible)*	*Minimum basin size (digital/photo)*	*Repeat period*
Aircraft			
orthophoto	3 m	1 km^2	As needed
Landsat			
TM	28.5 m	2.5/5 km^2	16 days
RBV	40 m	5/10 km^2	18 days
MSS	57 m	10/20 km^2	16 days
NOAA			
AVHRR	1.1 km	200/500 km^2	12 h
GOES			
VISSR	1.1 km	200/500 km^2	As needed

The algorithm for the snow/no-snow determinations are rather simple depending upon the type of data available. Patil *et al.* (1981) developed a simple algorithm for the Nimbus-7 satellite based on the simple difference of brightness temperatures at 18 and 37 GHz. Rango *et al.* (1979) reported an analogous differencing algorithm based on the horizontally polarized brightness temperature and the vertically polarized brightness temperature. Both approaches depend on the difference exceeding an empirically determined threshold to indicate snow cover.

The NOAA data set is known to have a number of shortcomings in areas with persistent cloud cover, low solar illumination, dense forest, patchy snow, and mountainous regions (Robinson *et al.,* 1993). However, the most important characteristic of the data set for studying snow-cover variability is that the analysis methodology has been relatively stable for over 25 years (Basist *et al.,* 1996). The passive microwave data are not limited by solar illumination or cloud cover, and offer a higher resolution. Like AVHRR, MODIS provides near-daily global coverage, but at spatial resolutions ranging from 250 m to 1 km. Only two channels in the visible and near-infrared spectral bands are available at 250-m resolution; five channels in the visible, near-infrared, and short-wave infrared are available at 500-m resolution, and the remaining 29 MODIS channels have a spatial resolution of 1 km, and may not be suitable for snow mapping because they were designed for use over ocean or atmosphere targets. MODIS has onboard visible/near-infrared calibrators while the AVHRR does not, thus it is able to derive radiances of snow using some of the MODIS sensors. At least one of the visible MODIS channels does not saturate over snow. This is an advancement over the AVHRR and TM sensors that experience significant saturation over snow and ice targets in the visible channels. The MODIS snow and ice products consist of 500-m or 1-km resolution binary maps of snow and ice cover, respectively, produced on a global, daily basis in most months (Hall *et al.,* 1995).

Development of subpixel analysis techniques (Gomes-Landesa, 1997) has allowed snow cover mapping on basins as small as 10 km^2 using the AVHRR data. This approach could make NOAA AVHRR data more widely useable for hydrological applications after it is tested in different geographic regions. Gomez-Landesa and Rango (2000) compared snow cover mapping of NOAA-AVHRR with the higher resolution (250 m pixel) data from the MODIS on NASA’s Terra satellite platform for the Noguera Ribagorzana Basin (572.9 km2) in the Central Pyrenees of Spain. The correlation between AVHRR and MODIS snow maps were on the order of 0.8–0.9 with good agreement between the snow distribution with altitude obtained from both instruments. The agreement was good even in very small basins with an area ~ 8.3 km^2.

The capability of remote sensing to provide areal coverage has resulted in a greater appreciation of the location of the snowpack in the basin. Even more important than the snow extent and location for various snowpack processes is the vertical dimension of the snowpack. This vertical dimension essentially provides the information needed for estimating snow volume which relates directly to the potential for snowmelt runoff. Although the capabilities for remote sensing of snow cover extent are more advanced and more simple, the remote sensing of snow depth or water equivalent has a very high potential.

4.2 SNOW DEPTH

The most straightforward way to measure snow depth from a remote platform is the survey of permanent aerial markers from light aircraft. These surveys provide accurate point measurements of snow depth, and many such measurements can be acquired in a short period of time. Other photogrammetric techniques have been used to measure snow depth by comparing the photos of the ground before snow cover is formed and after snow has been deposited. Snow depth is measured by subtracting photogrammetrically determined ground surface elevations from similar elevations of snow covered sample points. This approach can be used for both aircraft (Cooper, 1965) and ground based (Blyth *et al.,* 1974) surveys of snow depth.

From space, visible satellite imagery can be used to estimate snow depth in areas of relatively shallow snow accumulation of up to 25 cm (McGinnis *et al.,* 1975). They found a direct correlation between increasing brightness and increasing snow depth in areas without tall vegetation cover in the south-eastern U.S.A. This is a limited application that is relevant only in relatively flat areas soon after a snowfall. Natural reflectivity changes with time will affect the empirical relationship.

Passive microwave attempts at estimating snow depth have also been limited to flat areas because the poor resolution of the sensors prevents easy application in steep terrain. The studies that have been reported (Rango *et al.,* 1979; Foster *et al.,* 1980; Hall *et al.,* 1984; 1987) employ an empirical relationship between snow depth and microwave brightness temperature.

The positive results in these large flat areas show much promise for estimating the potential winter kill of wheat which is affected strongly by the depth of snow cover in these areas.

Recent passive microwave research based on theoretical concepts (Hallikainen 1984; Chang *et al.* 1987) has led to simple snow depth algorithms. Chang *et al.* (1987) assumed a snow density of 0.30 and a grain size of 0.35 mm to develop the following algorithm:

$$SD = 1.59[T_B(18H) - T_B(37H)] \tag{1.2}$$

where SD is the snow depth in centimeters, and $T_B(18H)$ and $T_B(37H)$ are the brightness temperatures for the SMMR 18 and 37 GHz horizontal polarization channels respectively.

4.3 SNOW WATER EQUIVALENT

Determination of density changes of snow and the presence of liquid water in the snow are very important to hydrologists because they are a common signal of incipient melt. The presence of liquid water in the snow *per se* does not change the spectral reflectance of snow. However, the process of metamorphosis that occurs during the snow season and is accelerated as the melt season approaches does have an effect on the albedo, primarily through the increase in the crystal size of the snow grains and through the accumulation of litter on the snow surface.

Snow water equivalence has been estimated by a residual method in which measured runoff data are used to reconstitute the snow water content (Martinec and Rango, 1981). Landsat data have been used on a grid basis to track the disappearance of snow and, concurrently, the degree days necessary to melt the snow are calculated. These results can be used to improve the areal distribution of snow water equivalent in the basin and to correct winter precipitation measurements.

Data for microwave model development and validation have been obtained from numerous truck and aircraft field experiments with a large number of these being carried out in Colorado (Chang *et al.,* 1979; 1984). Most of the satellite microwave studies for water equivalent estimation have been over large areas and of an empirical nature. Locations such as the high plains of the U.S.A., the Canadian high plains, the northslope of Alaska and the high plains or steppes of the CIS have been used for the satellite studies (Rango *et al.,* 1979; Goodison *et al.,* 1986). Rango *et al.* (1979) were also able to use the passive microwave data to monitor the buildup of the snowpack water equivalent from November to March in North Dakota for the 1975-6 snow season. Analysis of the Nimbus-7 SMMR data over mountainous terrain was successful to the extent that an empirical relationship between 18 and 37 GHz brightness temperature difference and 1 April snow water equivalent was derived for the 3419 km^2 Rio Grande basin in Colorado. The average snow water equivalent for the basin was predicted to within 15% of the actual value for both 1986 and 1987 (Rango *et al.,* 1989).

The general approach used to derive SWE and snow depth from passive microwave satellite data relates back to those presented by Rango *et al.* (1979) and Kunzi *et al.* (1982) using empirical approaches and Chang *et al.* (1987) using a theoretical basis from radiative transfer calculations to estimate snow depth from SMMR data. As discussed in Rott (1997), the most generally applied algorithms for deriving depth or SWE are based on the generalized relation given in Eq. (1.3)

$$SWE = A + B\frac{T_B(f_1) - T_B(f_2)}{f_2 - f_1} \tag{1.3}$$

in mm, for SWE > 0, where *A* and *B* are the offset and slope of the regression of the brightness temperature difference between a high scattering channel (f_2, commonly 37 GHz) and a low scattering one (f_1, commonly 18 or 19 GHz) of vertical or horizontal polarization. No single global algorithm will estimate snow depth or water equivalent under all snowpack and land cover conditions. The coefficients are generally determined for different climate and land covered regions and for different snow cover conditions; algorithms used in regions other than for which they were developed and tested usually provide inaccurate estimates of snow cover. In addition, accurate retrieval of information on snow extent, depth, and water equivalent requires dry snow conditions, because the presence of liquid water within the snowpack drastically alters the emissivity of the snow, resulting in brightness temperatures significantly higher than if that snowpack were dry. Therefore, an early morning overpass (local time) is the preferred orbit for retrieval of snow cover information to minimize wet snow conditions. It is also recognized that knowledge of snowpack state is useful for hydrological applications. Regular monitoring allows detection of the onset of melt or wet snow conditions.

A method has been developed in Finland which combines several different approaches to measuring or estimating snow water equivalent (Kuittinen, 1989). Ground based point measurements of water equivalent are made as usual about twice a month. One aerial gamma ray flight is made at the beginning of the snowmelt season to give line transect values of snow water equivalent. All available NOAA-AVHRR satellite images in the spring are used to provide areal snow water equivalent estimates based on a relationship between the percentage of bare spots in the snow cover and snow water equivalent. The point, line and areal snow water equivalent values are used with a method of correlation functions and weighting factors, as suggested by Peck *et al.* (1985), to determine an areal value based on all data. Evaluations in the Finland study have shown that the error of the estimate of areal snow water equivalent is less than 3-5 cm (Kuittinen, 1989).

4.4 OTHER SNOW PROPERTIES

After snow is deposited on the ground and a snowpack forms, the internal and surface characteristics of the snowpack change with time. This change, or snow metamorphism, is influenced by the snowpack energy balance, snow and air temperatures and vapour pressures, liquid water content and impurities deposited on the surface of the snow. Several processes normally take place. Large crystals or grains are normally reduced in size by destructive metamorphism which is primarily driven by vapour pressure gradients. As the winter season progresses, an increase in grain size through constructive metamorphism takes place, especially if a strong temperature gradient between the air (low) and snowpack (higher) sets up for a long period of time. As the melt season approaches, equitemperature metamorphism becomes dominant and individual grain sizes decrease but clusters of loosely bonded grains tend to form. Freeze and thaw cycles throughout the winter and spring seasons cause additional structures to form such as ice lenses or layers. Other natural changes with time are settling and compaction, increases in density and a reduction in albedo. Remote sensing monitoring of these changes can be accomplished to a certain degree by selecting the appropriate wavelength bands.

Grain sizes in the snowpack are difficult to measure by remote sensing. Microwave emission is strongly influenced by the grain size, as is shown by Chang *et al.* (1982). However, it is difficult to distinguish between different grain sizes and the number of snow grains. As yet there is no dependable way to quantify grain size with microwave measurements. Research with visible and near infrared reflectivities have established surface layer optical ice grain radii, but evidence is lacking on how this value relates to physical grain size (Dozier, 1987). The largest sensitivity of snow reflectance to grain size occurs in the near infra-red wavelengths (1.0-1.3 μm*)* where no current satellite sensors make measurements (Dozier, 1989). Future sensors such as the high resolution imaging spectrometer to be launched in connection with the space station in the 1990s will be able to take observations in the appropriate near infra-red bands. Our grain size measurement capability should increase with the launch of this instrument.

Detection of snowpack layering is possible using small portable microwave radar systems mounted on skis and pulled over the snow surface (or buried beneath the snowpack). The depth of the layers in the snowpack, based on the time of return of the reflected wave, can be extracted from the data (Gubler and Hiller, 1984). As data analysis techniques are perfected, similar active microwave wavelength measurements from space should be possible because of the inherent high resolution of radar.

The albedo of the snow surface changes with time as grain sizes change and surface impurities collect on the snow. Remote sensors only collect a small portion of the light reflected by the snow, i.e. the light reflected towards the sensor in the specific electromagnetic band of the sensor. The albedo, on the other hand, is made up of light reflected in all directions off the snow over all portions of the electromagnetic spectrum. As the bidirectional reflectance distribution function has not been investigated thoroughly, it is extremely difficult at present to take one remote sensing reflectance measurement and deduce the albedo from it. In a general way, we can say that the albedo decreases in the visible region as more impurities reach the snow surface and in the near infra-red as the size of individual grains or clusters of grains increase. As this is what happens as the snow season progresses, remote sensors see this general decrease in albedo with time. Remote sensing techniques, as yet, have not come up with the total bidirectional reflectance distribution function or albedo. Work such as that by Dozier *et al.* (1988) is necessary to eventually enable effective albedo measurements.

Two other changes associated with snow metamorphism can be monitored with remote sensing. The surface temperature of the snow can be measured with thermal infra-red wavelengths from various altitudes. Although the surface temperature cannot be used to reliably estimate temperature at depth in the snowpack, the variability of the surface temperature with time can provide some idea of the condition of the snowpack. As spring approaches the snowpack temperature remains at or near 0°C for longer periods of time. When the surface temperature persists at 0°C throughout the diurnal cycle, it can be inferred that the snowpack is at or near an isothermal condition. The capability of making measurements of surface temperature at least twice every 24 hours, such as with NOAA-AVHRR, is required. Associated with this isothermal condition is the appearance of liquid water in the snowpack as the snow starts to melt. As the microwave emission is greatly affected by liquid water, microwave techniques can be used to identify the initiation of melt metamorphism in the snowpack. As a result of the presence of liquid water, wet snow causes a higher dielectric loss in the microwave frequencies resulting in a high microwave emissivity much in excess of dry snow. A passive microwave radiometer measures a pronounced jump in the brightness temperature when even a small amount of liquid water is produced in a dry snowpack.

5. THE MOST POPULAR AND WIDELY USED SATELITE SNOW DATA SETS

5.1 NIMBUS-7 SMMR DERIVED GLOBAL MONTHLY SNOW COVER AND SNOW DEPTH (SMMR)

The Scanning Multichannel Microwave Radiometer operated on NASA's Nimbus-7 satellite (Chang *et al.,* 1982) for more than eight years, from 26 October 1978 to 20 August 1987, transmitting data every other day. Intended to obtain ocean circulation parameters such as sea surface temperatures, low altitude winds, water vapor and cloud liquid water content on an all-weather basis (Oakes *et al.,* 1989), the SMMR is a ten-channel instrument capable of receiving both horizontally and vertically polarized radiation. The instrument could deliver orthogonally polarized antenna temperature data at five microwave wavelengths, 0.81, 1.36, 1.66, 2.8 and 4.54 cm.

Beginning in November 1978, the Scanning Multichannel Microwave Radiometer (SMMR) on the Nimbus-7 satellite, with its capacity for penetrating clouds and snow packs, made it feasible to measure snow extent, calculate snow depth on an areal basis, and retrieve snow water equivalent regardless of weather or lighting conditions.

The global monthly averaged snow cover and snow depth maps produced for this data set were generated using the remotely sensed microwave signals has been developed by a group of NASA scientists (Chang *et al.,* 1979,1982,1984, 1987, 1991; Foster et al., 1984; Hall et al., 1984). Data are placed into ½ degree latitude by ½ degree longitude grid cells. SMMR data were interpolated for spatial and temporal gaps. Overlapping data in a cell from separate orbits within the same six-day period are averaged to give a single brightness temperature, assumed to be at the center of the cell. Maps are based on six-day average brightness temperature data from the middle week of each month. Oceans and bays are masked so that only microwave data for land areas are distinct.

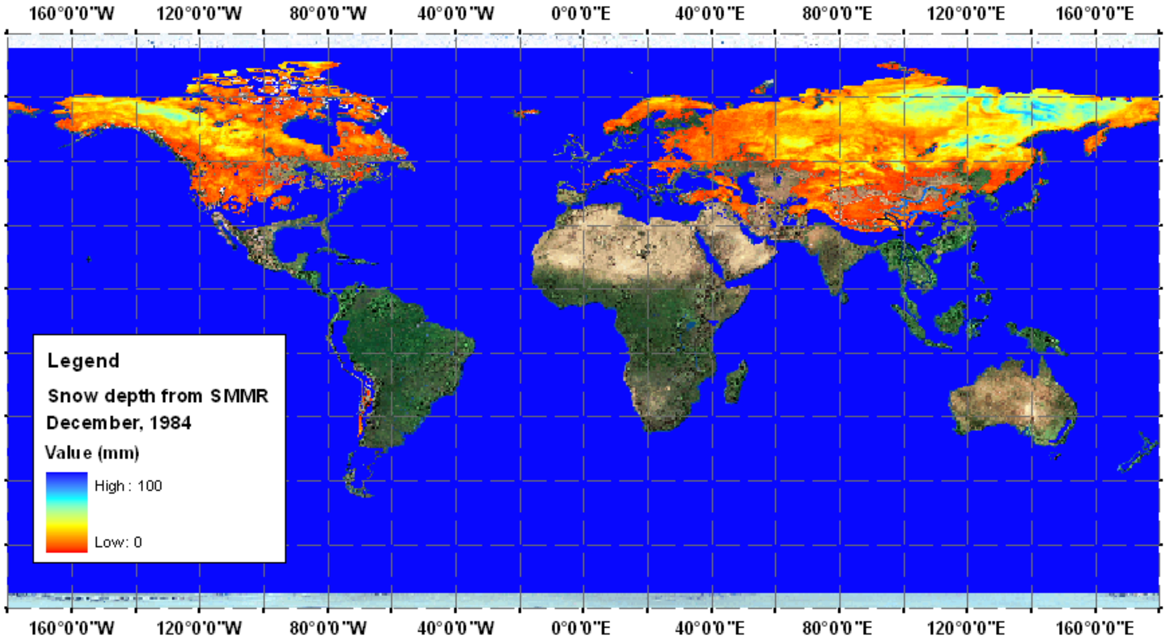

Fig. 1 Nimbus-7 SMMR global monthly map of snow depth for December, 1984

5.2 SSM/I DERIVED GLOBAL SNOW COVER (SMMI)

The Defense Meteorological Satellite Program (DMSP) Special Sensor Microwave/Imager (SSM/I) became operational in July 1987 on the F-8 satellite. Subsequent SSM/I's have been flown on the F- 10 (November 1990), F-11 (December 1991), F-12 (August 1994), F-13 (March 1995), F-14 (April 1997) and most recently, F-15 (January 2000) satellites. At present, NESDIS receives data from the F-13, F-14 and F-15 satellites. The SSM/I is a seven channel passive microwave radiometer operating at four frequencies (19.35, 22.235, 37.0, and 85.5 GHz) and dual-polarization (except at 22.235 GHz which is V-polarization only). It should be noted that the SSM/I will be replaced by an advanced sensor, the SSMIS (Special Sensor Microwave Imager Sounder) on the F-16 satellite, which was launched in October 2003 and is still undergoing an extensive calibration/validation by the Naval Research Laboratory. However, there should be little impact on the suite of hydrological products described here, as the primary channels used are very similar between the SSM/I and SSMIS (Grody, 1991; Grody *et al.,* 1996).

The SSM/I products are useful for evaluating the mean climate state, it's interannual and seasonal variations, and the detection of anomalies associated with ENSO and regional climatic variations. Researchers from the Cooperative Institute for Climate Studies (CICS) maintain a time series of the entire SSM/I archive, now entering it''s 23rd year, which includes data from

July 1987 to the present. Monthly average products are produced for precipitation, cloud liquid water, total precipitable water, snow cover, sea-ice cover, and oceanic surface wind speed.

The snow cover data is available in global fields for each month and week of the year over the period January 1988 to the latest available week. The resolution is approximately 30 Km. The data sets start at: 80 north and 180 west, the data moves eastward around the globe at 0.33 degrees resolution, before stepping 0.33 degree southward, and once again rotating around the globe, this pattern continues southward to 80 degrees.

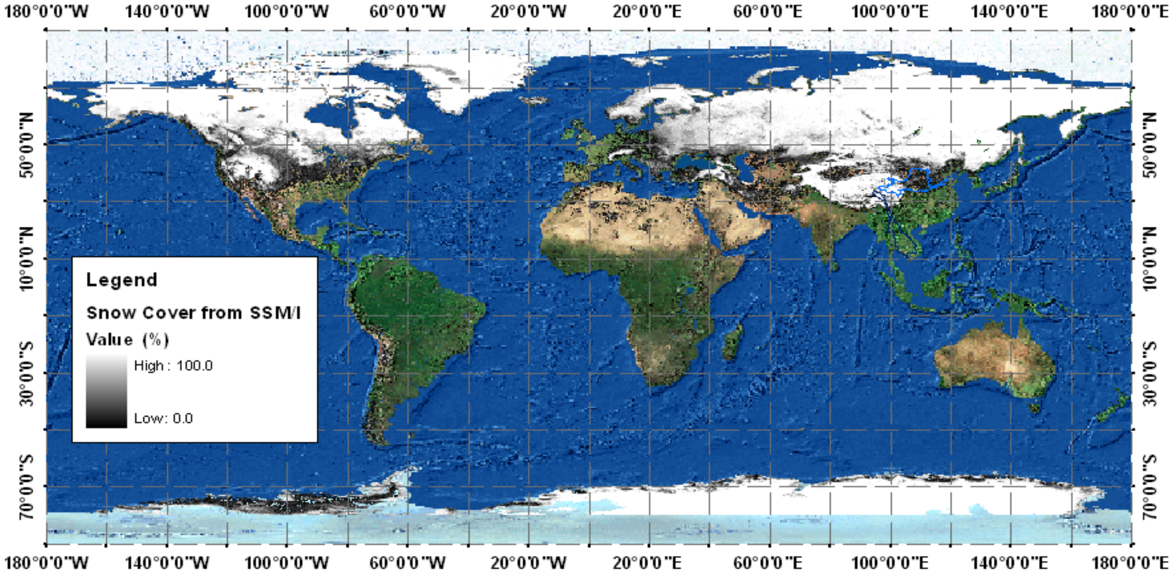

Fig. 2 SSMI global monthly map of snow cover distribution for December 1988.

5.3 GLOBAL MONTHLY EASE-GRID SNOW WATER EQUIVALENT CLIMATOLOGY

The Global Monthly Snow Water Equivalent Climatology data set comprises global, monthly satellite-derived snow water equivalent (SWE) climatologies from November 1978 through June 2003, with periodic updates released as resources permit. Global data are gridded to the Northern and Southern 25 km Equal-Area Scalable Earth Grids (EASE-Grids). Global snow water equivalent is derived from Scanning Multichannel Microwave Radiometer (SMMR) and selected Special Sensor Microwave/Imagers (SSM/I). Northern Hemisphere data are enhanced with snow cover frequencies derived from the Northern Hemisphere EASE-Grid Weekly Snow Cover and Sea Ice Extent Version 2 data (these data were not produced for the Southern Hemisphere).

This data set is derived from multiple sources. While the climatology files are gridded at 25-kilometer spatial resolution, the actual resolution of the component data (SWE or frequency of occurrence) depends on the input remote sensing data. The satellite passive microwave sensors at the frequencies used for these algorithms have sampling resolutions of 25 km, but the -3dB footprints vary by sensor and frequency, ranging from SMMR 18GHz at 55 x 41 km and SMMR 37 GHz at 27 x 18 km to both of the SSM/I frequencies re-sampled to the 19 GHz footprint at 69 x 43 km. The spatial resolution of the snow cover frequency of occurrence data derived from the Northern Hemisphere EASE-Grid Weekly Snow Cover and Sea Ice Extent Version 2 product ranges from 16,000 to 42,000 square kilometers (Armstrong et al., 2002).

Snow water equivalent data was derived from the following data sets: Nimbus-7 SMMR Pathfinder Daily EASE-Grid Brightness Temperatures and DMSP SSM/I Pathfinder Daily EASE-Grid Brightness Temperatures, and then was enhanced with Northern Hemisphere EASE-Grid weekly Snow Cover and Sea Ice Extent Version 2 data.

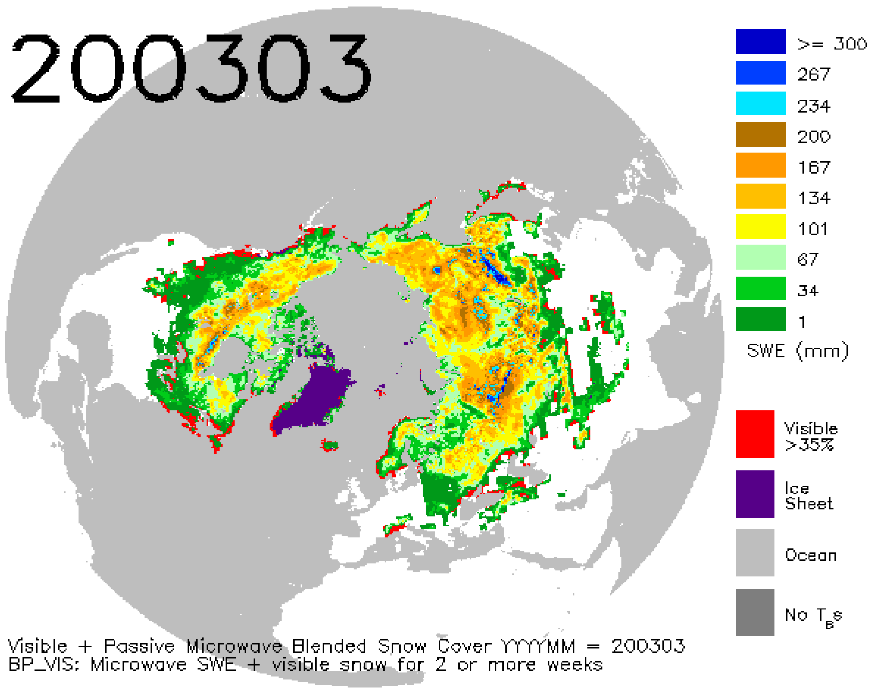

Fig. 3 GMSWEC map of the monthly averaged snow water equivalent (mm) in Northern Hemisphere for March 2003

5.4 MODIS SNOW PRODUCTS

The Moderate Resolution Imaging Spectroradiometer (MODIS) is a 36-channel visible to thermal-infrared sensor that was first launched as part of the Earth Observing System (EOS) Terra payload on 18 December 1999. A second MODIS was launched as part of the payload on the Aqua satellite on May 4, 2002. A variety of snow and ice products is produced from the MODIS sensors, and the products are available at a variety of spatial and temporal resolutions. The MODIS snow product suite begins with a 500-m resolution, 2330-km swath snow-cover map which is then gridded to a sinusoidal grid. The sequence proceeds to climate-modeling grid (CMG) products on a latitude/longitude (cylindrical equidistant projection). Most of the products are archived at the National Snow and Ice Data Center (NSIDC) in Boulder, CO.

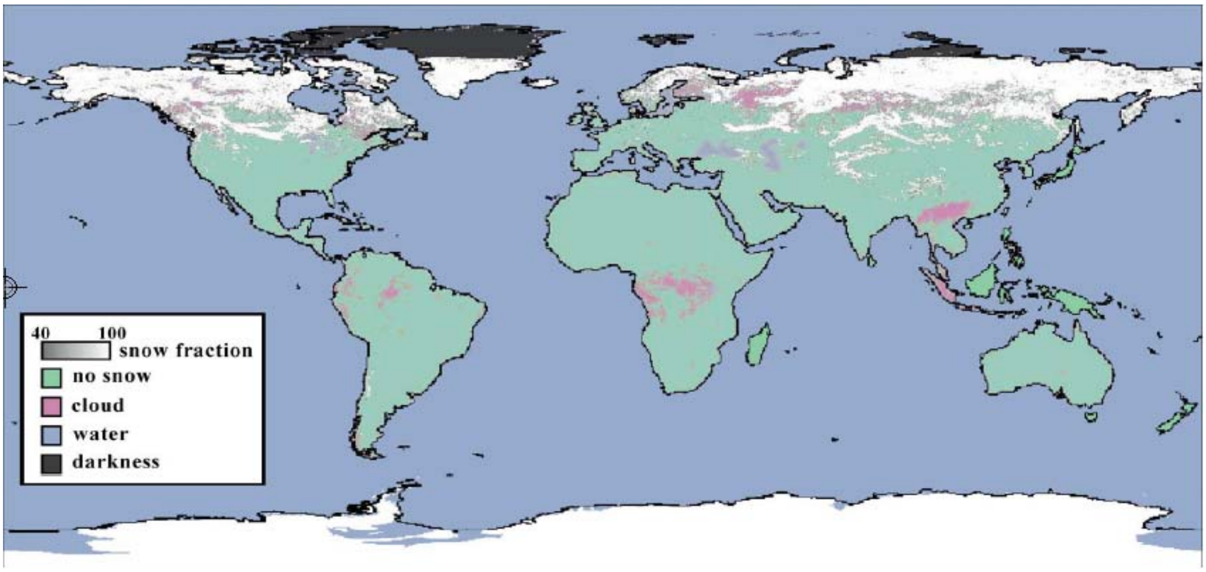

Рис. 4. 8-days composite global map of snow cover distribution MODIS (MOD10C2) March 6-13, 2002.

5.5 Advanced Microwave Scanning Radiometer (AMSR-E)

The Advanced Microwave Scanning Radiometer - Earth Observing System (AMSR-E) instrument on the NASA Earth Observing System (EOS) Aqua satellite provides global passive microwave measurements of terrestrial, oceanic, and atmospheric variables for the investigation of water and energy cycles, including precipitation rate, sea surface temperature, sea ice concentration, snow water equivalent, soil moisture, surface wetness, wind speed, atmospheric cloud water, and water vapor. These data products and related information are available on several websites including the site of National Snow and Ice Data Center (www.nsidc.org).

The list of Standard AMSR-E Data Products includes three Snow Water Equivalent (SWE) data sets, namely:

a. AMSR-E/Aqua Daily L3 Global Snow Water Equivalent EASE-Grids;
b. AMSR-E/Aqua 5-Day L3 Global Snow Water Equivalent EASE- Grids;
c. AMSR-E/Aqua Monthly L3 Global Snow Water Equivalent EASE-Grids.

These Level-3 Snow Water Equivalent (SWE) data sets contain SWE data and quality assurance flags mapped to Northern and Southern Hemisphere 25 km Equal-Area Scalable Earth Grids (EASE-Grids). Data are stored in Hierarchical Data Format - Earth Observing System (HDF-EOS) format, and are available from 19 June 2002 to the present.

The original baseline SWE algorithm is based on methods described in Chang, Foster, and Hall (1987) and Chang et al. (1997). This algorithm identifies land regions that are historically affected by snow; it retrieves the SWE using the simple brightness temperature difference approach described in Chang, Foster, and Hall (1987). Enhancements have been made to the original baseline algorithm including improved SWE retrieval methods (Kelly and Foster 2005) and (Kelly, Foster, and Hall 2005), and advancements will continue with ongoing algorithm updates.

Daily data are created by performing retrievals on individual AMSR-E Level-2A brightness temperature samples. The retrievals are then averaged to the 25 km Northern and Southern

Hemisphere EASE-Grid. The 5-day maximum SWE granules are created from daily data composites. Derived snow variables from the daily product over the same grid cell are screened for consistency based on statistical tests. Maximum SWE is recorded. Monthly averaged SWE granules are also created from daily data composites. Mean SWE is recorded.

References

Abbott, M.B., Bathurst, J.C., Cunge, J.A., O'Connell, P.E. and Rasmussen, J. (1986) An Introduction to the European Hydrological System - Système Hydrologique Européen, 'SHE'. *J. Hydrol.*, *Vol. 87*, pp. 45-77.

Anderson, E. A., (1968) Development and Testing of Snow Pack Energy balance equations, Water Resources Research, 4(1): 19-37.

Anderson, E. A., (1973), National Weather Service River Forecast System-Snow Accumulation and Ablation Model, NOAA Technical Memorandum NWS HYDRO-17, U.S. Dept of Commerce.

Anderson, E. A., (1976) A Point Energy and Mass Balance Model of a Snow Cover, NOAA Technical report NWS 19, U.S. Department of Commerce.

Anderson, E. A. and N. H. Crawford, (1964) The synthesis of continuous snowmelt hydrographs on a digital computer, Technical Report no 36, Stanford University Department of Civil Engineering.

Barry, R. G., Fallot, J. -M., and Armstrong, R. L. (1995) Twentieth-century variability in snow cover conditions and approaches to detecting and monitoring changes: status and prospects. *Prog. In Phys. Geog.*, **19**, 520-532.

Basist, A., D. Garrett, R. Ferraro, N. Grody, and K. Mitchell, (1996) A comparison between snow cover products derived from visible and microwave satellite observations. *J. Appl. Met.*, **35**, 163-177.

Bergström, S. (1975) The Development of a Snow Routine for the HBV-2 Model, *Nordic Hydrology*, Vol. 3: 73-92.

Beven, K.J. (1989) Changing Ideas in Hydrology – The Case of Physically-Based Models. *J. Hydrol.*, *Vol. 105*, pp. 157-172.

Bishop, R. and Watt, W. E. (1975) "SIMFLO—A Continuous Streamflow Simulation Model," Canadian Hydrology Symposium, Winnipeg, Canada.

Blöschl, G. (1999) Scaling Issues in Snow Hydrology. *Hydrol. Process., Vol. 13*, pp. 2149-2175.

Blöschl, G., and Sivapalan, M. (1995) Scale Issues in Hydrological Modelling - a Review. *Hydrol. Process., Vol. 9*, pp. 251-290

Blyth, K., Cooper, M. A. R., Lindsey, N. E., and Painter, R. B. (1974) Snow depth measurement with terrestrial photos, *Photogr. Engin.,* 40, 937-942.

Bowley, C. J., Barnes, J. C. and Rango, A. (1981) Applications systems verification and transfer project, vol. VIII: Satellite snow mapping and runoff prediction handbook. *NASA Tech. Pap.* 1829, Goddard Space Flight Center, Greenbelt, MD.

Bowling, L.C., and 23 others (2002). Simulation of high latitude hydrological processes in the Torne-Kalix basin: PILPS Phase 2e. 1: Experiment design and summary intercomparisons. Global and Planetary Change.

Bras, R. L., (1990), Hydrology, An introduction to hydrologic science, Addison-Wesley, Reading, MA.

Braun, L. (1985) Simulation of Snowmelt-Runoff in Lowland and Lower Alpine Regions of Switzerland. *Zuer. Geogr. Schriften,* Heft 21.

Brown, A. J., Hannaford, J. F. and Hall, R. L. (1979) Application of snow covered area to runoff forecasting in selected basins of the Sierra, Nevada, California. *Proc. Final Workshop on Operational Applications of Satellite Snow Cover Observations,* NASA CP-2116, pp. 185-200.

Brunt, D., (1952), Physical and Dynamical Meteorology, Cambridge University Press, Cambridge.

Brutsaert, W., (1975) On a derivable formula for long-wave radiation from clear skies, Water Resources Research, 11: 742-744. Brutsaert, W., (1982), Evaporation into the Atmosphere, Kluwer Academic Publishers, 299 p.

Carroll, S. S. and Carroll, T. R. (1989) Effect of forest biomass on airborne snow water equivalent estimates obtained by measuring terrestrial gamma radiation. *Remote Sensing Environ.* 7, 313-20.

Carroll, T. R. and Vadnais, K. G. (1980) Operational airborne measurement of snow water equivalent using natural terrestrial gamma radiation. *Proc. 48th Annu. Western Snow Conf., Laramie, WY,* Western Snow Conference, pp. 97-106.

Carroll, T. R. and Vose, G. D. (1984) Airborne snow water equivalent measurements over a forested environment using terrestrial gamma radiation. *Proc. 41st Annu. Eastern Snow Conf., New Carrollton, MD.,* Eastern Snow Conference, p. 19.

Castruccio, P. A., Loats, Jr, H. L., Lloyd, D. and Newman, P. B. (1980) Cost/benefit analysis for the operational applications of satellite snow cover observations (OASSO). *Proc. Final Workshop on Operational Applications of Satellite Snow Cover Observations,* NASA CP-2116, pp. 239-54.

Chang, A., Foster, J. and Hall, D. K. (1987) NIMBUS-7 derived global snow cover parameters. *Ann. Glaciol.* 9, 39-44.

Chang, A. T. C, Foster, J. L., Hall, D. K., Rango, A., and Hartline, B. K. (1982) Snow water equivalent estimation by microwave radiometry, *Cold Regions Res. Technol,* 5, 259-267.

Chang, A. T. C., Foster J. L., and Rango, A. (1991) Utilization of surface cover composition to improve the microwave determination of snow water equivalent in a mountainous basin. *Intl. J. Remote Sensing*, **12**, 2311-2319.

Chang, A. T. C, Rango, A., Shiue, J. C, Boyne, H., Farr, J., and Brown, K. (1984) Preliminary results from the Pingree Park, Colorado passive microwave experiment during January and March, 1981, *Document X-924-84-15,* Goddard Space Flight Center, Greenbelt, MD, 9pp.

Chang, A. T. C, Shiue, J. C., Boyne, H., Ellerbruch, D., Counas, G., Wittman, R., and Jones, R. (1979) Preliminary results of passive microwave snow experiment during February and March, 1978, *NASA Technical Paper No. 1408,* NASA, Washington DC, 109pp.

Christopherson, R.W. (2003) Glacial and periglacial processes and landforms. In *Geosystems: An Introduction to Physical Geography*. 5th ed. Prentice Hall, New Jersey: 519-553.

Church, J.A., J.M. Gregory, et al. (2001) Changes in sea level. In *Climate Change 2001: The Scientific Basis.* Working Group I, Intergovernmental Panel on Climate Change (IPCC): 639-693.

Colbeck, S. C., (1978), The physical aspects of water flow through snow, Advances in Hydroscience, 11.

Colbeck, S. C., (1991), The layered character of snow covers, Reviews of Geophysics, 29(1): 81-96.

Cooper, C. F. (1965) Snow cover measurement, *Photogr. Engin.* 31, 611-619.

Crane, R. G. and Anderson, M. R. (1984) Satellite discrimination of snow/cloud surfaces. *Int. J. Remote Sensing* 5, 213-23.

Cully, K.M. and S.J. Marshall (2000) Substantial contribution to sea-level rise during the last interglacial from the Greenland ice sheet. *Nature*. 404: 591-594.

Dey, B., Goswami, D. C. and Rango, A. (1983) Utilization of satellite snow-cover observations for seasonal streamflow estimates in the western Himalayas. *Nord. Hydrol.* 257-266.

Dingman, S.L. (2002) Physical Hydrology, 2nd ed., Prentice-Hall, Inc.

Dillard, J. P. and Orwig, C. E. (1979) Use of satellite data in runoff forecasting in the heavily forested, cloud covered Pacific northwest. *Proc. Final Workshop on Operational Applications of Satellite Snow Cover Observations,* NASA CP-2116, pp. 127-150.

Dozier, J., (1979) A Solar Radiation Model for a Snow Surface in Mountainous Terrain, in Proceedings Modeling Snow Cover Runoff, ed. S. C. Colbeck and M. Ray, U.S. Army Cold Reg. Res. Eng. Lab., Hanover, NH, p.144-153.

Dozier, J. (1984) Snow reflectance from Landsat-4 thematic mapper. *IEEE Trans. Geosci. Remote Sensing* **GE-22,** 323-8.

Dozier, J. (1987) Recent research in snow hydrology, *Rev. Geophys.,* 25, 153-161.

Dozier, J. (1989) Spectral signature of alpine snow cover from the Landsat Thematic Mapper, *Remote Sens. Environ.,* 28, 9-22.

Dozier, J., Davis, R. E., Chang, A. T. C, and Brown, K. (1988) The spectral bidirectional reflectance of snow', *Spectral Signatures of Objects in Remote Sensing, Fourth International Colloquium, ESA SP-287,* European Space Agency, Paris, pp. 87-92.

Dozier, J. and J. Frew, (1990) Rapid Calculation of Terrain Parameters for Radiation Modeling From Digital Elevation Data, IEEE Transactions on Geoscience and Remote Sensing, 28(5): 963-969.

Dozier, J. and Marks, D. (1987) Snow mapping and classification from Landsat Thematic Mapper. *Ann. Glaciol.* 9, 97-103.

Dubayah, R., J. Dozier and F. W. Davis, (1990) Topographic Distribution of Clear-Sky Radiation Over the Konza Prairie, Kansas," Water Resources Research, 26(4): 679-690.

Engman, E. T. and Gurney R. J. (1991) *Remote Sensing in Hydrology.* Chapman and Hall, London.

Essery, R., Martin, E., Douville, H., Fernandez, A., and Brun, E. (1999) A comparison of four snow models using observations from an alpine site. *Clim. Dyn.*, *Vol. 15*, pp. 583-593.

Ferguson, R.I. (1999) Snowmelt Runoff Models, *Progress In Physical Geography*, Vol. 23 (2), pp. 205-227.

Frew, J. E., (1990) The Image Processing Workbench, PhD Thesis, Geography, University of California, Santa Barbara.

Foster, J. L., Hall, D. K. and Chang, A. T. C. (1987) Remote sensing of snow. *Eos* 68(32), 681-4.

Foster, J. L., Hall, D. K., Chang, A. T. C. and Rango, A. (1984) An overview of passive microwave snow research and results. *Rev. Geophys. Space Phys.* 22, 195-208.

Foster, J. L., Rango, A., Hall, D. K., Chang, A. T. C, Allison, L. J., and Diesen, B. C. (1980) Snowpack monitoring in North America and Eurasia using passive microwave satellite data, *Remote Sens. Environ.,* 10, 285-298.

Ghate, S. R., and Whiteley, H. R. (1977) Gawser Model User's Manual, School of Engineering, University of Guelph, Guelph, Ontario, Canada, Technical Report: 126-137.

Glynn, J. E., Carroll, T. R., Holman, P. B. and Grasty, R. L. (1988) An airborne gamma ray snow survey of a forest covered area with a deep snowpack. *Remote Sensing Environ.* 26, 149-60.

Gohin, F., A. Cavanié, and R. Ezraty (1998), Evolution of the passive and active microwave signatures of a large sea ice feature during its 2½-year drift through the Arctic Ocean. *J. Geophys. Res.* 103(C4): 8,177-8,189.

Gomez-Landesa E. (1997) Evaluacion de Recursos de Agua en Forma de Nieve mediante Teledeteccion usando satelites de la sine NOAA (Evaluation of water resources in the form of snow by remote sensing using NOAA satellites). PhD thesis, Universidad Politenica de Madrid, Madrid, Spain.

Gomez-Landesa E., Rango A. (2000) Assessment of MODIS channels 1and 2 snow cover mapping capability. EOS Trans Am Geophy Union 2000; 81(48):F548.

Goodison, B. E., (1989) Determination of areal snow water equivalent on the Canadian prairies using microwave radiometry. *Proc. IGARSS'89*, Vancouver, July 1989, **3**, 1243-1246.

Goodison, B. E., Rubinstein, I., Thirkettle, F. W., and Langham, E. J. (1986) Determination of snow water equivalent on the Canadian prairies using microwave radiometry, *Modelling Snowmelt-Induced Processes (Proceedings of the Budapest Symposium), IAHS Publ. No. 155,* pp. 163-173.

Granger, R.J., and D.H. Male (1978) "Melting of a Prairie, Snowpack", J. Appl. Meteorol. (now J. Clim. Appl. Meteorol.) vol. 17, no. 2, pp. 1833-1842.

Gray, D. M., and Prowse, T. D. (1992) Snow and Floating Ice, in *Handbook of Hydrology*, D. R. Maidment, ed., McGraw-Hill, Inc., New York: 7.1-7.58.

Gray, D. M. and D. H. Male, ed. (1981), Handbook of Snow, Principles, processes, management & use, Pergamon Press.

Griggs, M. (1968) Emissivities of natural surfaces in the 8- to 14-micron spectral region. *J. Geophys. Res.* 73, 7545-51.

Gubler, H. and Hiller, M. (1984) The use of microwave FMCW radar in snow and avalanche research, *Cold Regions Sci. Technol,* 9, 109-119.

Gurtz, J., Zappa, M., Jasper, K., Lang, H., Verbunt, M., Badoux, A., and Vitvar, T. (2001) A Comparative Study in Modelling Runoff and its Components in Two Mountainous Catchments. *In Hydrol. Process.*

Hall, D. K. and Martinec, J. (1985) *Remote Sensing of Ice and Snow,* Chapman and Hall, London.

Hall, D. K., Chang, A. T. C., and Foster, J. L. (1987) Seasonal and interannual observations and modeling of the snowpack on the arctic coastal plain of Alaska using satellite data, *Proceedings of the Cold Regions Hydrology Symposium,* American Water Resources Association, Fairbanks, AL, pp. 521-529.

Hall, D. K., Foster, J. L., and Chang, A. T. C. (1984) Nimbus-7 SMMR polarization responses to snow depth in the mid-western U.S., *Nordic Hydrol,* 15, 1-8.

Hall, D. K., G. A. Riggs, and V. V. Salomonson, (1995) Development of methods for mapping global snow cover using moderate resolution imaging spectroradiometer data. *Rem. Sens. of Environ.*, **54**, 127-140.

Hallikainen, M. (1984) Retrieval of snow water equivalent from NIMBUS-7 SMMR data: Effect of land cover categories and weather conditions. *IEEE J. Ocean Eng.* **OE-9,** 372-6.

Hallikainen, M. and Jolma, P. (1986) Development of algorithms to retrieve the water equivalent of snow cover from satellite microwave radiometer data. In: Proc 1986 International Geoscience and Remote Sensing Symposium (IGARSS 86), Zurich, Switzerland. pp. 611–616.

Hendrick, R. L., B. D. Filgate and W. M. Adams, (1971) Application of Environmental Analysis to Watershed Snowmelt, Journal of Applied Meteorology, (10): 418-429.

Hildore, J.J. and J.E. Oliver (1993) Polar and highland climates. In *Climatology: An Atmospheric Science*. Macmillan Publishing Co., New York: 327-346.

Hock, R (2001) Evaluation and recent developments in temperature-index melt modelling in mountain regions. *J. Hydrol.*

Johanson, R. C., et al. (1984) "User's Manual for Hydrological Simulation Program, FORTRAN (SHP-F)," EPA 600/9-80-015, U.S. EPA, Athens, GA.

Kawata, Y., Kusaka, T. and Veno, S. (1988) Snowmelt runoff estimation using snowcover extent data and its application to optimum control of dam water level. *Proc. IGARSS'88 Symp. Edinburgh, Scotland,* ESA SP-284, pp. 439-40.

Kirnbauer, R., Blöschl, G., and Gutknecht, D. (1994) Entering the Era of Distributed Snow Models, *Nordic Hydr*ology, *Vol. 25*, pp. 1-24.

Kite, G. W. (1978) Development of a Hydrologic Model for a Canadian Watershed, *Canadian Journal of Civil Engineering*, Vol. 5: 126.

Klemeš, V. (1990) The Modelling of Mountain Hydrology: the Ultimate Challenge, *Hydrology of Mountainous Areas*, L. Molar, Ed. *IAHS*, *Vol. 190*, pp. 29-43.

Klok, E.J., Jasper, K., Roelofsma, K.P., Badoux, A., and Gurtz, J. (2001) Distributed hydrological modelling of a glaciated Alpine river basin. *Hydrological Sciences Journal*, *Vol. 46*, pp. 553-570.

Kondo, J. and T. Yamazaki, (1990) A prediction model for snowmelt, snow surface temperature and freezing depth using a heat balance method, Journal of applied meteorology, 29: 375-384.

Kuittinen, R. (1989) Determination of snow water equivalents by using NOAA-satellite images, gamma ray spectrometry and field measurements, *Remote Sensing and Large-Scale Global Processes (Proceedings of the Third International Assembly, Baltimore), IAHS Publ. No. 186,* pp. 151-159.

Kunzi, K. F., Patil, S. and Rott, H. (1982) Snow-covered parameters retrieved from NIMBUS-7 SMMR data. *IEEE Trans. Geosci. Remote Sensing* **GE-20,** 452-67.

Kuzmin, P. P., (1961), Protsess Tayaniya Shezhnogo Pokrova (Melting of Snow Cover), [English translation by Israel Prog. Sci. Transl., Transl. 71].

Lang, H., and Braun, L. (1990) On the Information content of air Temperature in the Context of Snow Melt Estimation, *Hydrology of Mountainous Areas*, L. Molar, Ed. *IAHS*, *Vol. 190*, pp. 347-354.

Leaf, C. F. (1969) Aerial photographs for operational streamflow forecasting in the Colorado Rockies. *Proc. 37th Western Snow Conf, Salt Lake City, UT.*

Leaf, C. F. and Brink, G. E. (1973) Hydrologic simulation model of Colorado subalpine forest. *USDA Forest Service, Res. Pap.* RM-107, Fort Collins, CO.

Leavesley, G. H. (1973) A Mountain Watershed Simulation Model: Fort Collins, Colorado, Colorado State University, Ph. D. dissertation.

Leavesley, G. H., R. W. Lichty, B. M. Troutman and L. G. Saindon, (1983) Precipitation-runoff modeling system--Users manual, Water resources Investigations Report 83-4238, U.S. Geological Survey.

Leavesley, G. H., A. M. Lumb and L. G. Saindon, (1987) A microcomputer-based watershed modeling and data-management system, in 55th Annual meeting, Western Snow Conference, April 14-17, p.108-117.

Leu, C. H., (1988) Evaluation of Spatially-Distributed snowpack estimation using pattern recognition, PhD Thesis, Civil and environmental engineering, Utah State University.

Linsley, R. K., M. A. Kohler and J. L. H. Paulhus, (1975) Hydrology for Engineers, 2nd Edition, McGraw-Hill, Kogakusha, Ltd.

Logan, L. A. (1976) A Computer-Aided Snowmelt Model for Augmenting Winter Streamflow Simulation in a Southern Ontario Drainage Basin, *Canadian Journal of Civil Engineering*, Vol. 3: 531.

L’vovich, M.I. (1974) *World Water Resources and Their Future*. Translated by R.L. Nace, Washington DC: Amerial Geografical Union.

Marks, D. and J. Dozier, (1979) A Clear-Sky Longwave Radiation Model for Remote Alpine Areas, Archev Fur Meteorologie Geophysik und Bioklimatologie, Ser B, 27: 159-187.

Marshall, S. E. and S. G. Warren, (1987) Parameterization of snow albedo for climate models, in Large Scale Effects of Seasonal Snowcover, Proceedings of the Vancouver Symposium, August 1987, IAHS Publ. no. 166.

Martinec, J., (1960) Degree-Day Factor for Snowmelt Runoff Forecasting, Int. Union Geodesy Geophys. Gen. Assembly of Helsinky, Int. Assoc. Hydrol. Sci. Comm. Surface Waters, IAHS Publ. 51, pp. 468-477.

Martinec, J. (1975) Snowmelt-runoff model for streamflow forecasts. *Nord. Hydrol.* 6, 145-54.

Martinec, J. and Rango, A. (1981) Areal distribution of snow water equivalent evaluated by snow cover monitoring. *Water Resour. Res.* 17, 1480-8.

Martinec, J., Rango, A. and Major, E. (1983) *The Snowmelt-Runoff Model (SRM) User's Manual.* NASA Ref. Publ. 1100, Washington, DC.

Martinec, J. and Rango, A. (1986) Parameter values for snowmelt runoff modeling. *J. Hydrol.* 84, 197-219.

Matson, M., (1991) NOAA satellite snow cover data. *Paleogeography and Paleoecology*. 90:213-280.

Matson, M., Roeplewski, C.F., and Varnadore, M.S. (1986) An Atlas of Satellite-Derived Northern Hemisphere Snow Cover Frequency. National Weather Service. Washington D.C., 75 p.

Matzler, C. and Schanda, E. (1983) Snow mapping with active microwave sensor. *January Report*. University of Berne, Institute of Applied Physics, Berne.

McGinnis, D. F., Pritchard, J. A. and Wiesnet, D. R. (1975) Determination of snow depth and snow extent from NOAA-2 satellite very high resolution radiometer data. *Water Resour. Res.* 11, 892-902.

McKay, G.A. (1963) Relationships between Snow Survey and Climatological Measurements, Int. Union Geod. Georphys. Gen. Assem. Berkeley (Surface Water), *Int. Assoc. Hydrol. Sci., Publ.* 63, pp. 214-227, 1963.

Morris, E. M., (1982) Sensitivity of the European Hydrological System snow models, in Hydrological Aspects of Alpine and High Mountain Areas, Proceedings of the Exeter Symposium, IAHS Publ no 138, p.221-231.

Morris, E. M. (1983) Modeling the Flow of Mass and Energy Within a Snowpack for Hydrological Forecasting, *Annals of Glaciology,* Vol. 4: 198-203.

Morris, E. M, and Godfrey, J. (1978) The European Hydrological System Snow Routine, *Proceedings: Modeling of Snow Cover Runoff*, S. C. Colbeck and M. Ray, ed., U.S Army Cold Regions Research Engineering Laboratory, Hanover, NH: 269-278.

National Snow and Ice Data Center (NSIDC) (date of publication unknown), All about glaciers. http://nsidc.org/glaciers. Accessed on 1 December 2003a.

National Snow and Ice Data Center (NSIDC) (date of publication unknown), All about snow. http://nsidc.org/snow. Accessed on 1 December 2003b.

National Snow and Ice Data Center (NSIDC) (date of publication unknown), State of the cryosphere. http://nsidc.org/sotc. Accessed on 1 December 2003d.

Nicholls, R.J. (2002), Rising sea levels: potential impacts and responses. *Issues in Environmental Science and Tech.* 17: 83-107.

Ohmura, A. (2001) Physical Basis for the Temperature-Based Melt-Index Method, *J. Appl. Meteor*., Vol. 40, pp. 753-761.

Ontario Ministry of Natural Resources (1989) *Snow Hydrology Guide,* Published by Ministry of Natural Resources, Queen's Park, Ontario, Canada.

Ostrem, G., Andersen, T. and Odegaard, H. (1981) Operational use of satellite data for snow inventory and runoff forecast. *Satellite Hydrology,* American Water Resources Association, Minneapolis, MN, pp. 230-4.

Patil, S. Kunzi, K. F. and Ron, H., (1981) The global snow cover seen by the NIMBUS-7 Scanning Multichannel Microwave Radiometer (SMMR). *Proc. 11th Eur. Microwave Conf, Amsterdam,* Microwave Exhibitions and Publications, Amsterdam, The Netherlands, pp. 227-32.

Peck, E. L., Johnson, E. R., Keefer, T. N., and Rango, A. (1985) Combining measurements of hydrological variables of various sampling geometries and measurement accuracies, *Hydrological Applications of Remote Sensing and Remote Data Transmission (Proceedings of the Hamburg Symposium), IAHS Publ. No. 145,* pp. 591-599.

Price, A. G. and T. Dunne, (1976), Energy balance computations of snowmelt in a subarctic area, Water Resources Research, 12(4): 686-694.

Quick, M. C., and Pipes, A. (1977) UBC Watershed Model, *Hydrological Sciences Bulletin*, Vol. XXII, No. 1: 153.

Ramamoorthi, A. S. (1983) Snowmelt run-off studies using remote sensing data, *Proc. Indian Acad. Sci.,* 6, 279-286.

Ramamoorthi, A. S. (1987) Snow cover area (SCA) is the main factor in forecasting snowmelt runoff from major river basins, *Large Scale Effects of Seasonal Snow Cover (Proceedings of the Vancouver Symposium), IAHS Publ. No. 166,* pp. 187-198.

Ramsay, B.H., (1998) The interactive multi-sensor snow and ice mapping system. *Hydrological Processes*. 12:1537-1546.

Rango, A. (1980) Operational applications of satellite snow cover observations. *Water Res. Bull.* 16, 1066-73.

Rango, A. (1983) Application of a simple snowmelt-runoff model to large river basins. *Proc. 51st Western Snow Conf.* Western Snow Conference, pp. 89-99.

Rango, A. (1985) Results of the snowmelt-runoff model in an international test. *Proc. 53rd Western Snow Conf., Boulder, Co.,* Western Snow Conference, pp. 99-106.

Rango, A. (1993) Snow hydrology processes and remote sensing. *Hydrological Processes.* 7(2), pp. 121-138.

Rango, A., Chang, A. T. C. and Foster, J. L. (1979) The utilization of spaceborne microwave radiometers for monitoring snowpack properties. *Nord. Hydrol.* 10, 25-40.

Rango, A. and Itten, K. (1976) Satellite potentials in snowcover monitoring and runoff prediction. *Nord. Hydrol.* 7, 209-30.

Rango, A. and Martinec, J. (1979) Application of a snowmelt-runoff model using Landsat data. *Nord. Hydrol.* 10, 225-38.

Rango, A., Martinec, J., Chang, A. T. C, Foster, J. L., and van Katwijk, V. F. (1989) Average areal water equivalent of snow in a mountain basin using microwave and visible satellite data, *IEEE Trans. Geosci. Remote Sens.,* 27, 740-745.

Rango, A., Martinec, J., Foster, J. and Marks, D. (1983) Resolution in operational remote sensing of snow cover. *Hydrological Applications of Remote Sensing and Remote Data Transmission, Proc. Hamburg Symp., August, 1983, IAHS Publ. No.* 145, pp. 371-82.

Rango, A., Salomonson, V. V. and Foster, J. L. (1977) Seasonal streamflow estimation in the Himalayan region employing meteorological satellite snow cover observations. *Water Resour. Res.* 13, 109-12.

Riley, J. P., D. G. Chadwick and J. M. Bagley, (1966) Application of electronic analog computer to solution of hydrologic and river basin planning problems: Utah simulation model II, PRWG32-1, Utah Water research lab., Utah State University.

Robinson, D. A., K. F. Dewey, and R. R. Heim, (1993) Global snow cover monitoring: an update. *Bull. Amer. Meteorol. Soc.*, **74**, 1689-1696.

Rott, H. (1986) Prospects of microwave remote sensing for snow hydrology. *Hydrological Applications of Remote Sensing and Remote Data Transmission (Proceeding of the Hamburg Symposium)*. *IAHS Publ. No. 145*, pp. 361-369.

Rott H. (1997) Capabilities of micorwave sensors for monitoring areal extent and physical properties of the snowpack. In: Sorooshian S, Gupta HV, Rodda SC, editors. Land surface processes in hydrology. NATO ASI series on global environmental change, vol. 46. Berlin: Springer-Verlag; p. 135–67.

Satterlund, D. R., (1979) An Improved Equation for Estimating Long-wave Radiation From the Atmosphere," Water Resources Research, 15: 1643-1650.

Shafer, B. A. and Leaf, C. F. (1979) Landsat derived snowcover as an input variable for snowmelt runoff forecasting in Central Colorado. *Proc. Final Workshop on Operational Applications of Satellite Snow Cover Observations,* NASA CP-2116, pp. 151-69.

Slater, A.G., Schlosser, C.A., Desborough, C.E., Pitman, A.J., Henderson-Sellers, A., Robock, A., Vinnikov, K.Ya., Mitchell, K. and the PILPS 2(d) Contributors (2001): The Representation of Snow in Land-surface Schemes; Results from PILPS 2(d). *J. Hydrometeorology*, **2**, 7-25

Small, C. and R.J. Nicholls (2003), A global analysis of human settlement in coastal zones. *J. Coastal Res.* 19(3): 584-599.

Stiles, W.H., Ulaby, F.T., and Rango, A. (1981) Microwave measurements of snow pack properties. *Nordic Hydrol.* **12**, pp. 143-166.

Tarboton, D.G. and Luece, M.S. (1997) Utah Energy Balance Snow Accumulation and Melt Model (UEB), Computer model technical description and users guide, Utan Water Research Laboratory, Logan, Utah.

Thomas, R.H., et al. (2001) Program for Arctic Regional Climate Assessment (PARCA): goals, key findings, and future directions. *J. Geophys. Res.* 106(D24): 33,691-33,705.

U.S. Army Corps of Engineers, (1956) Snow Hydrology, Summary report of the Snow Investigations., U.S. Army Corps of Engineers, North Pacific Division, Portland, Oregon.

US Army Corp of Engineers, Runoff from Snowmelt (1960) (EM 1110-2-1406):68, Washington, DC. US Govt Printing.

U.S. Army Corps of Engineers (1990) “HEC-1 Flood Hydrograph Package, User's Manual,” Hydrologic Engineering Center, Davis, CA.

U.S. Army Corps of Engineers (1991) “User Manual, SSARR Model, Streamflow Synthesis and Reservoir,” North Pacific Division.

Vershinina, L. K. (1985) The use of aerial gamma surveys of snowpack for spring snowmelt runoff forecasts. *Hydrological Applications of Remote Sensing and Remote Data Transmission, Proc. Hamburg Symp, August 1983, IAHS Publ. No.* 145, pp. 411-20.

Viessman, W., G. L. Lewis and J. W. Knapp, (1989) Introduction to Hydrology, 3rd Edition, Harper & Row.

Wilson, Walter T., (1941) An outline of the thermodynamics of snowmelt, Am. Georphys. Union Trans., part 1:182-195.

Wiscombe, W. J. and S. G. Warren, (1981) A Model of the Spectral Albedo of Snow. I: Pure Snow, Journal of the Atmospheric Sciences, 37: 2712-2733.

World Meteorological Organization (1982) WMO project for the intercomparison of conceptual models of snowmelt runoff. *Hydrological Aspects of Alpine and High Mountain Areas, Proc. Exeter Symp., IAHS Publ. No.* 138, pp. 193-202.

WMO (1986) Intercomparison of models of snowmelt runoff. Operational Hydrology Report 23, World Meteorological Organization, Geneva.

Young, R. A., G. R. Benoit and C. A. Onstad, (1989) Snowmelt and frozen soil, Chapter 3 in USDA Water Erosion Prediction Project, Hillslope profile model documentation, Edited by L. J. Lane and M. A. Nearing, NSERL Report #2, USDA-ARS National Soil Erosion Research Laboratory, West Lafayette, Indiana, 47907.